Mon. Not. R. Astron. Soc. **262,** 128–140 (1993)

# The Type II supernova 1988Z in MCG + 03-28-022: increasing evidence of interaction of supernova ejecta with a circumstellar wind★

M. Turatto,[1,2] E. Cappellaro,[1] I. J. Danziger,[2] S. Benetti,[3] C. Gouiffes[2] and M. Della Valle[4]

[1] *Osservatorio Astronomico di Padova, vicolo dell'Osservatorio 5, I-35122 Padova, Italy*
[2] *European Southern Observatory, Karl-Schwarzschild-Strasse 2, D-8048 Garching, Germany*
[3] *Dipartimento di Astronomia, Università di Padova, vicolo dell'Osservatorio 5, 1-35122 Padova, Italy*
[4] *European Southern Observatory, Casilla 19001, Chile*

Accepted 1992 October 20. Received 1992 October 20; in original form 1992 May 20

**ABSTRACT**

We present a set of optical observations of SN 1988Z covering a period of 3 yr from the discovery. This relatively bright supernova shows an unusual photometric behaviour, with broad light curves in the *B*, *V* and *R* bands resembling those of SN 1987F. The colour evolution is unique, with a slow blueward evolution in the early months, after which it remains nearly constant. The spectrum is characterized at all epochs by strong Balmer emission, without the usual P Cygni absorption component which is typical of SNeII at early stages. Several He I emission lines are also visible. These lines have a complex structure, with several components evolving with time with respect to both width and intensity. The H$\alpha$ luminosity decline is exceptionally slow and cannot be explained by a simple radioactive model, so this object is an ideal candidate for a supernova in which there is interaction of the SN ejecta with a circumstellar wind. A number of unresolved, forbidden emission lines of [O III], [N II], [Ne III], [Fe II], [Fe III], [Fe VII], [Fe X] and, tentatively, of [Fe XI], [A X] and [Ca V] have been identified. Their presence and relative strengths suggest the existence of a shock, which gives further support to the theory of an ejecta–wind interaction.

**Key words:** shock waves – techniques: photometric – techniques: spectroscopic – circumstellar matter – supernovae: individual: 1988Z.

## 1 INTRODUCTION

The sole unifying characteristic of Type II supernovae (SNeII), accepted by common consent, is the presence of the Balmer lines in their spectra; the general spectral appearance and the luminosity evolution can vary dramatically. Although several attempts have been made to allot different SNeII to homogeneous families, the definition of these subclasses is not unanimously accepted.

Although there are other supernovae with properties akin to those of SN 1988Z, this object falls among the most extreme cases of Type II.

SN 1988Z was discovered at Asiago by Candeo on December 12.0 UT, 11 arcsec east and 2 arcsec south of the nucleus of MGC + 03-28-022 (Cappellaro & Turatto 1988) and about 2.7 arcsec south and 0.9 arcsec east of a bright knot (Fig. 1). The SN was independently detected by Pollas (1988) two days later. The parent galaxy is not classified in the major catalogues and appears on our frames as a barred advanced-type spiral (SBc), seen nearly pole-on. Most of the other objects present on the frames are galaxies, probably members of a background cluster.

At discovery, the SN was already too faint to be followed spectroscopically in Asiago with the equipment available at that time. For this reason, we did not obtain adequate spectroscopic coverage of the early stages of the evolution of the SN. With the start of the ESO Key-Program on Supernovae (Turatto et al. 1990a), the SN became one of the most interesting targets with the large telescopes. Later, the upgrading of the spectroscopic facilities, together with the slow fading rate of the SN, allowed its late detection again at Asiago.

★Based on observations collected at the European Southern Observatory at La Silla (Chile) and Asiago (Italy).

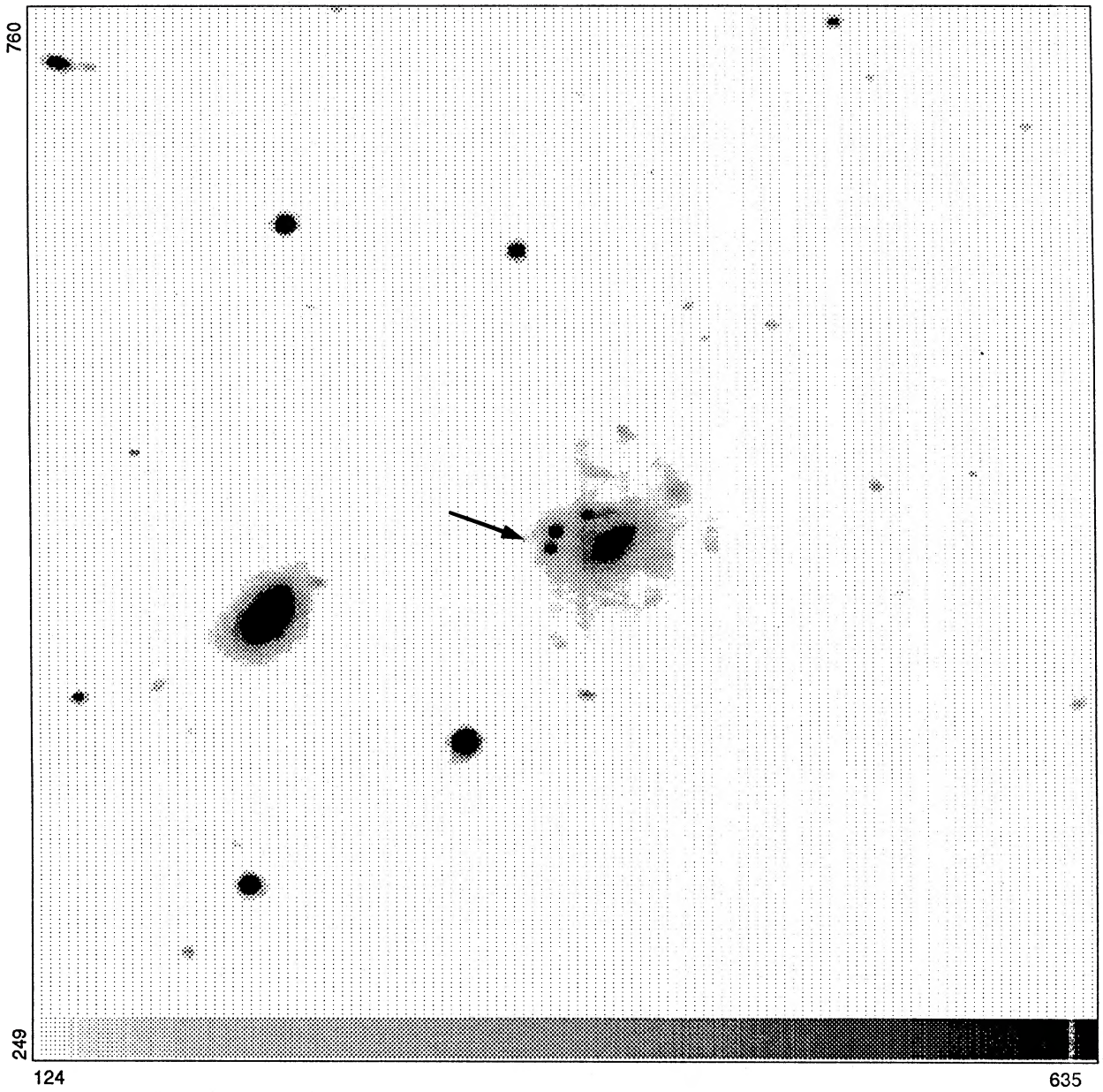


**Figure 1.** Red image of SN 1988Z in MCG+03-28-022 obtained on 1991 February 18 with EFOSC at the 3.6-m telescope. North is up and east to the left. The SN is located 11 arcsec east and 2 arcsec south of the nucleus of the parent galaxy and 2.7 arcsec south of a bright knot.

The following section (Section 2) gives a summary of the material collected jointly at the two observatories. In Sections 3 and 4 the photometric and spectroscopic data are discussed and compared to those of other prototypical SNeII. An interpretation of the observations in the light of the recent theoretical works on the subject is briefly given in Section 5. Conclusions are presented in Section 6.

## 2 THE OBSERVATIONS

The observations of SN 1988Z reported here (Table 1) extend over more than 3 yr. During this period, several telescopes and techniques (column 6 of the table) were used. The discovery plate and a number of early observations were obtained in Asiago with the 67/92-cm Schmidt telescope. Kodak 103a-O and 103a-D plates with GG13 and GG14 filters, respectively, were used to match the $B$ and $V$ bands. In these cases, the magnitudes were estimated by eye with reference to a comparison sequence of surrounding CCD-calibrated stars. According to our experience, these estimates have an uncertainty of about $\pm 0.1$ mag.

Most of the photometric observations were obtained both at La Silla and at Asiago with CCD detectors. In all cases, they were calibrated using a number of Landolt's (1983) standard stars. In order to allow longer exposure times at the larger telescopes, the frames were slightly defocused, thus reducing the errors in the calibration due to shutter timing. For each telescope, the computed colour terms were found

**Table 1.** Optical photometry of SN 1988Z.

| date | J.D. | B | V | R | tel. |
|---|---|---|---|---|---|
| 9/3/88 | 47230 | >19 | | | S67 |
| 8/4/88 | 47260 | >18 | | | S40 |
| 12/12/88 | 47508 | 16.75 | | | S67 |
| 14/12/88 | 47510 | 16.80 | 16.39 | 16.05 | 1.8 |
| 16/12/88 | 47512 | 16.80 | | | S67 |
| 4/1/89 | 47531 | 16.92 | 16.78: | 16.54: | 1.8 |
| 5/1/89 | 47532 | 16.90 | | | S67 |
| 31/1/89 | 47558 | 17.05 | | | S67 |
| 3/2/89 | 47561 | 17.25 | 16.95 | | S67 |
| 7/3/89 | 47593 | 17.65 | | | S67 |
| 9/3/89 | 47595 | 17.86 | 17.69 | | Dan |
| 5/4/89 | 47622 | 18.14 | 18.03 | | 3.6 |
| 6/4/89 | 47623 | | 17.90 | 17.59 | 3.6 |
| 8/4/89 | 47625 | | 18.07 | | 3.6 |
| 28/4/89 | 47645 | 18.24 | 17.90 | 17.65 | Dan |
| 29/12/89 | 47890 | | 19.18 | 17.92 | 1.8 |
| 23/1/90 | 47915 | | 19.50 | 18.17 | 1.8 |
| 26/2/90 | 47949 | 19.68 | 19.28 | 18.22 | Dan |
| 26/2/90 | 47949 | | | 18.17 | 1.8 |
| 8/3/90 | 47959 | | 19.35 | | NTT |
| 31/3/90 | 47982 | | | 18.21 | 1.8 |
| 13/12/90 | 48239 | 20.99 | 20.32 | | Dan |
| 18/12/90 | 48244 | | 20.41 | | 3.6 |
| 25/12/90 | 48251 | 21.00 | 20.25 | 19.00 | Dan |
| 10/1/91 | 48267 | | | 18.94 | 3.6 |
| 18/2/91 | 48306 | 21.10 | 20.40 | 19.06 | 3.6 |
| 20/2/91 | 48308 | | | 19.23 | 3.6 |
| 6/4/91 | 48353 | 21.50 | 20.77 | 19.20 | Dan |
| 3/12/91 | 48594 | | 20.98 | 19.65 | 1.8 |
| 12/12/91 | 48603 | | 20.75 | 19.60 | 1.8 |
| 3/2/92 | 48656 | 21.68 | 21.05 | 19.88 | 3.6 |

S67 = Asiago - Schmidt 67/92/200 cm + photographic plate; S40 = Asiago - Schmidt 40/60/100 cm + photographic plate; 1.8 = Asiago - 1.8-m telescope + CCD camera; 3.6 = ESO - 3.6-m telescope + EFOSC1; Dan = Danish/ESO - 1.5-m telescope + CCD; NTT = ESO - NTT + EFOSC2.

to be similar to values obtained previously by other observers with the same telescope–detector configurations. The SN magnitude determinations were performed interactively with the ROMAFOT package in MIDAS, which, in our experience, is very efficient for the measurement of faint objects on complex backgrounds or crowded fields. This code also allowed the careful subtraction of the contribution of the nearby northern knot (Fig. 1). Typical errors of the photometry were 0.05 mag at maximum, rising to 0.2 mag for the latest observations.

In the journal of the spectroscopic observations (Table 2) we give, for each spectrum, the equipment used (column 3), the exposure time (column 4) and the observed wavelength range (column 5). The extended range of the EFOSC1 spectra has been obtained by combining the B300 and R300 grisms. Two exposure times are therefore listed. Sometimes spectra taken a few days apart were added in order to reach higher signal-to-noise ratios. In these cases, column 4 shows the cumulative exposure times.

In spite of the different instrumentation used, the resulting resolution is always about 20 Å. All spectra were calibrated in wavelength with adjacent spectra of comparison lamps and were flux-calibrated with spectrophotometric standard stars observed on the same night as the SN. When the SN broad-band photometry was available on the same night, the absolute flux calibrations of the spectra were checked. These were in good agreement, to within a few tenths of magnitude.

**Table 2.** Journal of spectroscopic observations.

| Date | phase (days) | equipment | exp (min.) | range (Å) |
|---|---|---|---|---|
| 5-8/4/89 | 115 | 3.6m+EFOSC1 | 90/30 | 3600-9330 |
| 1/3/90 | 444 | 1.8m+B&C | 60 | 3570-7900 |
| 9/3/90 | 452 | NTT+EFOSC2 | 30 | 4535-7260 |
| 12-13/4/90 | 486 | 1.8m+B&C | 110 | 3640-7900 |
| 18/4/90 | 492 | 3.6m+EFOSC1 | 20/20 | 3530-10100 |
| 10-11/10/90 | 667 | 1.8m+B&C | 55 | 4750-9000 |
| 27/10/90 | 684 | 1.8m+B&C | 90 | 4800-9200 |
| 29/11/90 | 717 | 1.8m+B&C | 75 | 4565-8880 |
| 14/12/90 | 732 | 1.8m+B&C | 60 | 4565-8880 |
| 20/12/90 | 738 | 3.6m+EFOSC1 | 70 | 3550-7130 |
| 9-10/1/91 | 758 | 1.8m+B&C | 180 | 4620-8770 |
| 13/2/91 | 793 | 1.8m+B&C | 120 | 5375-9200 |
| 18-20/2/91 | 798 | 3.6m+EFOSC1 | 90/60 | 3725-9960 |
| 20-21/3/91 | 828 | 2.2m+B&C | 165 | 3920-9320 |
| 4/2/92 | 1149 | 3.6m+EFOSC1 | 100/60 | 3600-9650 |

## 3 THE PHOTOMETRY

### 3.1 The light and colour curves

A first discussion of the photometric properties of SN 1988Z was presented by Stathakis & Sadler (1991, hereafter SS) based on a few photometric measurements. We add here a significant number of *B*, *V* and *R* magnitudes. Fig. 2 shows the complete light curves in the three bands, including previously published data. When the fact that the SN was relatively faint is taken into account, the agreement with the data of other authors is very good.

From the available data, it is difficult to establish whether the SN was discovered near to maximum. Certainly we know that it was not visible on two plates taken in the late spring of 1988 (Table 1). However, considering the high intrinsic luminosity of the SN (see Section 3.2), it is probable that the maximum occurred not long before its early detection (JD 2447508) at $B_{max} \leq 16.8$, $V_{max} \leq 16.4$ and $R_{max} \leq 16.1$. Throughout this paper, all phases will refer to this date. Note that this is 11 d later than the reference date adopted by SS.

From the discovery, the SN fades monotonically at an unusually slow rate. In the first two months, the slopes of the light curves are $\beta_B = 0.74$, $\beta_V = 0.85$ and $B_R = 0.75$ mag $(100\ \mathrm{d})^{-1}$. Later, the three curves steepen slightly until about 110 d past maximum but never match those of other classical SNeII. It is of particular interest to compare (Fig. 3) the shape of the light curve of SN 1988Z with those of other SNeII: SN 1987A, the *linear* SN 1979C, the *plateau* SN 1969L and the peculiar SN 1987F. The photometric evolution of SN 1988Z is clearly slower than that of the other SNeII. A recent extensive study of the morphology of SNeII light curves (Patat 1992) showed that the light curve of SN 1988Z is matched only by that of SN 1987F.

Completely unmatched, however, is the colour evolution of SN 1988Z (shown in Fig. 4). In all SNeII studied previously (including SN 1987F), the light curves at shorter wavelengths are steeper than the redder ones in the first months after maximum. Fig. 4 reveals that the temporal evolution of

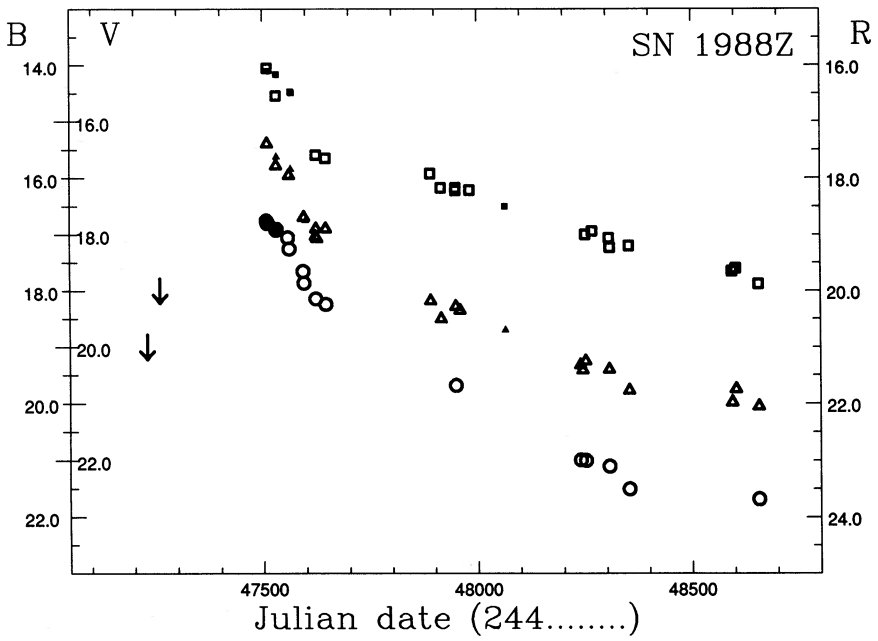


**Figure 2.** The light curves of SN 1988Z in the *B* (circles).*V* (triangles) and *R* (squares) bands. Open symbols represent measurements presented in this paper while small, filled symbols represent data from the literature. The two vertical arrows are *B* upper limits.

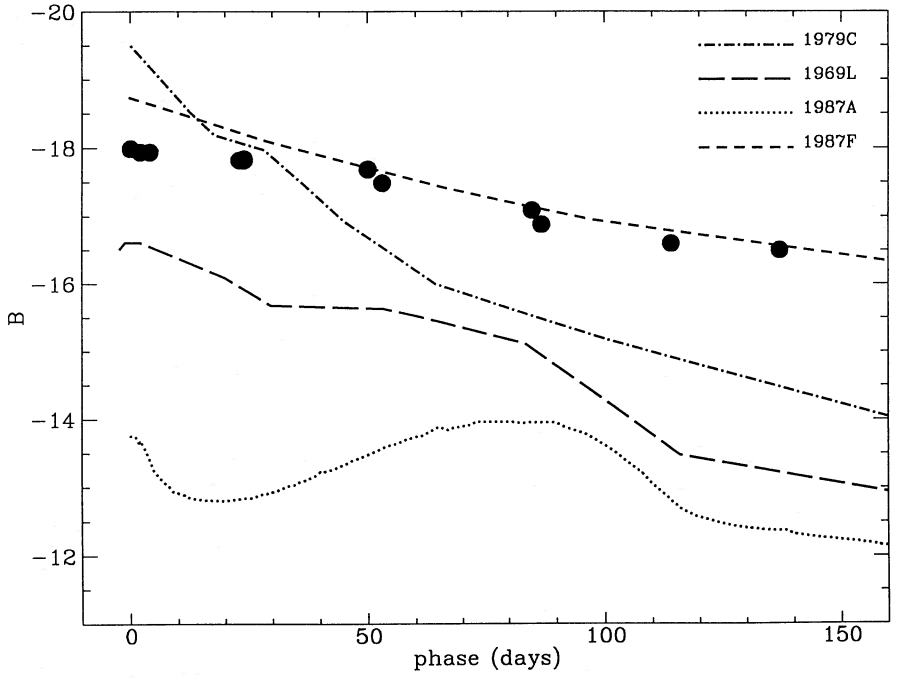


**Figure 3.** Comparison between the *absolute* blue light curve of SN 1988Z (dots) and the schematic light curves of other prototypical SNeII: SN 1969L (Ciatti, Rosino & Bertola 1971), SN 1979C (Barbon et al. 1982), SN 1987A (Whitelock 1991)and SN 1987F (Filippenko 1989). The curves are not corrected for possible absorption inside the parent galaxy.

$(B-V)$ for SN 1988Z displays the opposite tendency. For the first 100 d, the colour decreases from the initial value $(B-V)=0.4$ to $(B-V)\simeq 0.1$. The SN then becomes redder until about 700 d. Subsequently the colour remains nearly constant at $(B-V)\simeq 0.6-0.7$.

The late-time light curves of SN 1988Z are also very interesting. Turatto et al. (1990b) studied the decline rates of the light curves of SNe between 150 and 400 d past maximum. For SNeII, the decline rates are independent of the morphology of the early light curves and are in agree-

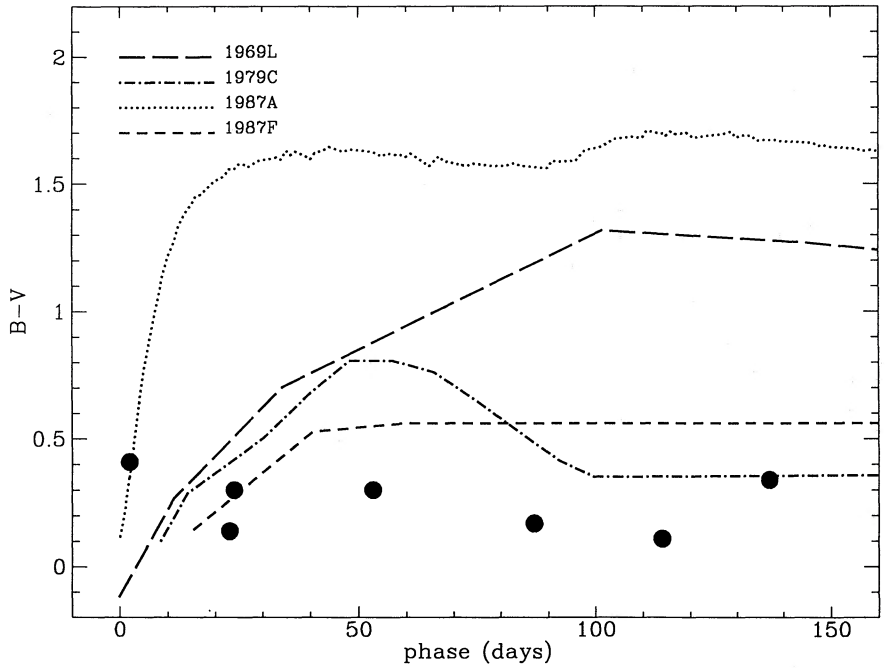


**Figure 4.** The colour evolution of SN 1988Z. For comparison, the colour curves of the SNe mentioned in Fig. 3 are drawn.

**Table 3.** Decline rates of SN 1988Z in the *B*, *V* and *R* bands.

| interval (days) | B | V | R |
|---|---|---|---|
| | mag/100$^d$ | | |
| 0–60 | 0.74 | 0.85 | 0.75 |
| 110–450 | 0.47 | 0.44 | 0.18 |
| 400–850 | 0.43 | 0.31 | 0.26 |
| 730–1150 | 0.15 | 0.16 | 0.20 |

ment with those expected from the radioactive decay of $^{56}$Co. The average values $\gamma_B = 0.74$ and $\gamma_V = 0.89$ mag $(100\ \mathrm{d})^{-1}$ have small dispersions ($\sigma_B = 0.11$, $\sigma_V = 0.04$), and the slopes of the three SNeII observed in the red, SN 1986I, SN 1987A (cf. Turatto et al. 1990b) and SN 1988A (Benetti, Cappellaro & Turatto 1991), are between 0.99 and 1.17 mag $(100\ \mathrm{d})^{-1}$. The corresponding decline rates of SN 1988Z are dramatically slower (cf. row 2 of Table 3).

After 400 d, only SN 1987A has been extensively studied. The SN is seen to fade very quickly in the optical, while the 10- and 20-μm fluxes begin to increase (Danziger et al. 1989; Lucy et al. 1989; Suntzeff & Bouchet 1990; Bouchet, Danziger & Lucy 1991) as a consequence of thermal emission following dust formation. The optical light curves then gradually level off, approaching the decline rate of $^{57}$Co ($\gamma_{^{57}\mathrm{Co}} = 0.28$ mag $(100\ \mathrm{d})^{-1}$).

The photometry of SN 1988Z covers over 3 yr. Up to 850 d, no significant change in the slopes is visible in *B* and *V*, while in *R* a steepening is perceivable after 400 d, when the slope becomes $\gamma_R = 0.26$ mag $(100\ \mathrm{d})^{-1}$. After this epoch, the three light curves become flatter with quite similar slopes (Table 3).

Whether additional sources of energy are implied, e.g. a pulsar or other radioactive isotopes such as $^{44}$Ti and $^{22}$Na [$\gamma_{^{44}\mathrm{Ti}} = 0.004$, $\gamma_{^{44}\mathrm{Na}} = 0.02$ mag $(100\ \mathrm{d})^{-1}$], and whether the contribution of an underlying background starts to be significant, cannot be determined on the basis of these data. This problem is aggravated by the fact that a bolometric light curve has not been measurable because of the faintness of the object.

### 3.2 The absolute magnitude

With the radial velocity at the location of the SN (see Section 4.3) and adopting $H_0 = 75$ km s$^{-1}$ Mpc$^{-1}$, the distance modulus of MGC+03-28-022 corresponds to $\mu = 34.77$. The galactic extinction in the direction of the SN is, according to Burstein & Heiles (1978), $A_B = 0$ and interstellar lines are not visible in the spectra. Moreover, the fact that the colour reaches relatively blue values suggests that the extinction within the parent galaxy is not strong. Thus from the blue apparent magnitudes of the SN at maximum, as discussed in the previous section, we obtain an absolute value of $M_B \leq -18.0$.

Since the dispersion of the absolute magnitudes of SNeII at maximum is very large ($M_{B,\max} = -16.89$ and $\sigma = 1.35$; Miller & Branch 1990), SN 1988Z, though brighter than average, is not exceptional in this respect. Patat (1992) showed that there are a number of SNeII, both linear and plateau, more luminous than SN 1988Z.

The situation is different 200 d later. Turatto et al. (1990b) showed that SNe with different properties at maximum have the same luminosity after 200 d. This property does not hold for SN 1988Z. Even if our light curve has a gap at this phase, it is clear that, because of its slow fading rate, SN 1988Z is at least 2 mag brighter than *normal*

SNe. Again, SN 1987F has a similar behaviour. In fact, because of the similarity in the shape of the light curves, SN 1987F has a comparable luminosity at this stage to that of SN 1988Z.

It is a point of curiosity to note that 3 yr after the discovery the absolute luminosity of SN 1988Z is still comparable to that of SN 1987A at maximum.

## 4 SPECTROSCOPY

The first spectra of SN 1988Z, taken within a week of the discovery, show a blue featureless continuum and several narrow nebular emission lines of H$\alpha$, H$\beta$, H$\gamma$, [O II], [O III], He I and He II, which are indicators of high temperature (Heathcote, Cowley & Hartwick 1988; Zamorano 1988; Filippenko 1991). There are no lines showing the P Cyg profile typical of SNeII at early stages.

The early spectral evolution can be followed in the sequences presented in Filippenko (1991) and SS. The continuum dominating the spectra becomes increasingly blue up to about 100 d, and this explains the behaviour of the colour curve (Section 3.1). One month after the discovery, the narrow emission lines start to broaden. At two months, a broad component (FWHM ~ 2000 km s$^{-1}$) is visible at H$\beta$ and H$\alpha$, the latter with another even broader component (FWHM ~ 15 000 km s$^{-1}$).

As early as day 62 (and possibly day 34), and very apparent on our spectra at day 115 (Fig. 5), is a blue excess pseudo-continuum extending from <3600 Å to 5700 Å. Apart from the identifiable narrow emission lines super-

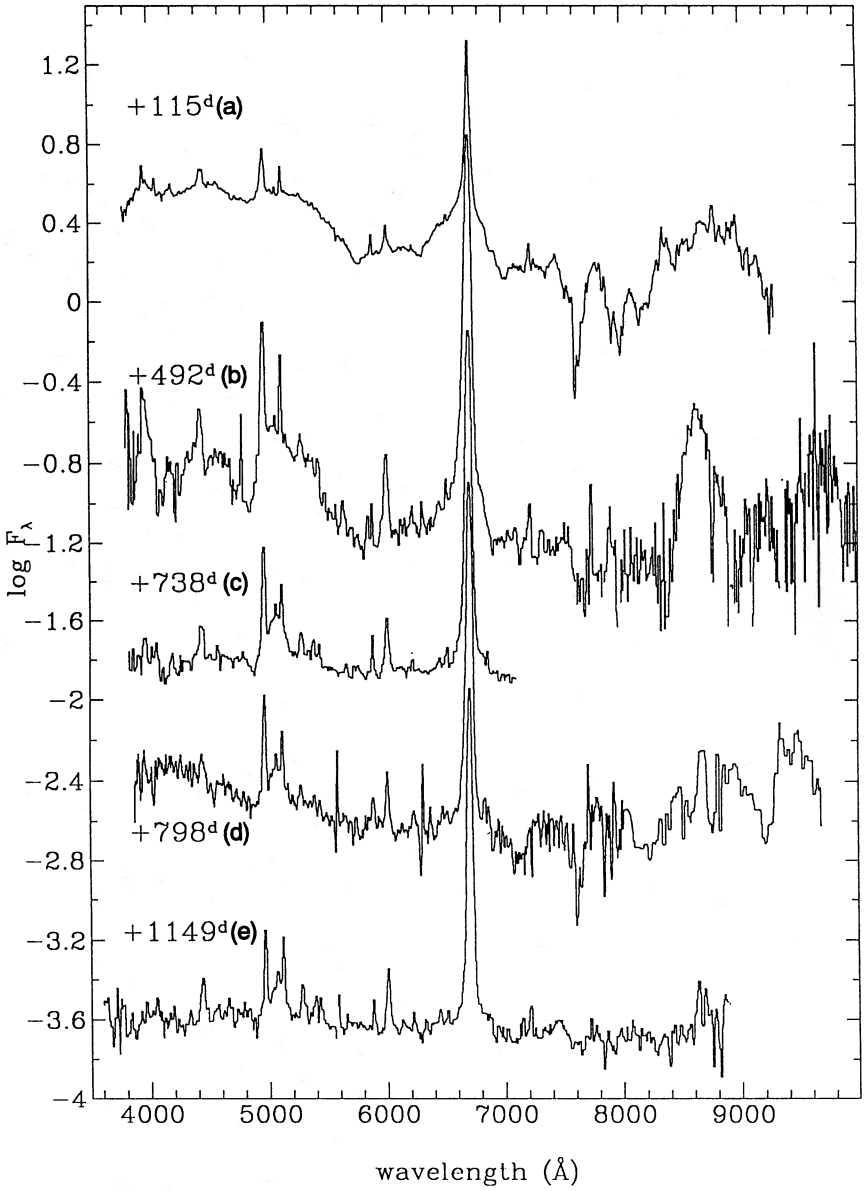


**Figure 5.** The spectral evolution of SN 1988Z on the EFOSC1 spectra (cf. Table 2). The ordinate scale is log $F_\lambda$, where fluxes are in $10^{-16}$ erg s$^{-1}$ cm$^{-2}$ Å$^{-1}$, and the observed wavelength is on the abscissa. Spectra (b), (c), (d) and (e) have been down-shifted by 0.7, 1.3, 2.1 and 2.8, respectively.

imposed on it, this pseudo-continuum, which is not without structure, may originate from the overlap of many neighbouring emission lines broadened in the expanding envelope of the supernova (this has also been suggested by SS). This feature remains to be explained and modelled. Forbidden and permitted lines of Fe II and Fe III may be expected to contribute significantly to this excess emission without necessarily accounting for all of it.

Of the spectra obtained at La Silla and Asiago which describe the evolution starting 115 d after the discovery, the most significant are presented in Fig. 5.

The presence of an underlying continuum is clear only in the day 115 spectrum, all other spectra being dominated by emission lines.

### 4.1 The systemic radial velocity

From the narrow emission lines of the SN spectrum at phase 115 d, a radial velocity $v = 6740$ km s$^{-1}$ is derived. This is very close to the velocity of the northern knot ($v = 6719$ km s$^{-1}$), whose spectrum shows only narrow H$\alpha$ + [N II] on a bright continuum, and is consistent with the velocity of the nuclear region of the parent galaxy ($v = 6667$ km s$^{-1}$), which emits bright narrow emission lines of H$\alpha$ + [N II], [S II], [O III] and H$\beta$. In the following, the first value ($v = 6740$ km s$^{-1}$) has been adopted as the rest frame of the SN.

### 4.2 The line identification

Many emission lines, most persisting for more than 2 yr, have been identified in those of our spectra with higher signal-to-noise ratios.

The first spectrum (115 d) is dominated by the Balmer lines of hydrogen, which are visible up to H8, whose shape and intensity will be discussed later. These lines and those of He I have both broad and narrow components.

The He II 4686-Å line seen in absorption in the early spectra is no longer visible in the first spectrum because the temperature near the photosphere has dropped. A narrow emission line is also apparent at early phases. Other lines include those of Ca II, possibly [Fe II] and, at later phases, O I. As well as the usual forbidden lines of [O III] and [N II], we identify narrow coronal lines of [Fe VII], [Fe X] and, more tentatively, of [Fe XI], [A X] and [Ca V].

Other lines of [Ne III], [Fe II] and [Fe III] probably contribute to some blends. Unlike other SNeII, the [O I] 6300- and 6363-Å lines and the [Ca II] 7291- and 7324-Å lines are absent, as was also noted by SS.

Fig. 6 shows many of these identifications. In Table 4, all the recognized emission lines at four different epochs are reported. The ions and the relative rest wavelengths are listed in columns 1 and 2. The shape of the lines is reported in column 3, while in columns 4, 5, 6, 7 and 8 are given the measured wavelengths, in the SN rest frame, for the five spectra respectively. The corresponding intensities are listed in columns 9–13.

#### *4.2.1 The O I line*

The redder part of the day 115 spectrum is dominated by a broad emission, centred at about 8700 Å. This is probably due to the IR Ca II triplet, while a contribution from O I 8446 Å is not excluded. The signal-to-noise ratio in this region is quite poor and the narrow spikes visible redward of 7500 Å are probably due to fringing that is not completely removed by the flat-fielding. At phase 492 d, only a narrower O I line is visible, in good agreement with the corresponding spectrum of SS, while the Ca II triplet has disappeared. At 1150 d after the discovery, the O I line is still present. The presence of this line, along with the absence of the O I 7774-Å line, is an indication that the 8446-Å line is not formed by recombination. It has been suggested that the mechanism producing the line is Ly$\beta$ pumping (Grandi 1980). This suggestion is supported by the large width of the O I line, which indicates that oxygen and hydrogen are emitted in the same region (cf. Section 4.2.3). This large width may subsequently be useful in modelling the region in which the line is formed. A pumping mechanism of this kind has been proposed to explain the presence of the O I 1.128-μm line in the spectrum of SN 1987A (Oliva, Moorwood & Danziger 1987).

#### *4.2.2 The He I lines*

Recombination lines of He I are present. Although most of the lines are weak or blended, the He I line shows a distinct two-component structure. The narrower component is unresolved and the FWHM of the broader component, once deconvolved for the instrumental resolution, gives an expansion velocity $v_{\mathrm{He\,I}} \simeq 2300$ km s$^{-1}$, which remains constant up to 1150 d (Table 5). Even though He I lines are uncommon in Type II SNe, they were detected in the late-time spectra of another unusual object, SN 1986J in NGC 891 (Rupen et al. 1987).

The line-intensity ratios of the He I lines change with time but remain, within the errors of the spectrophotometry, in agreement with the measurements by SS. In no case do the ratios fit those of case B recombination with $T = 5000$–$20\,000$ K and $N_e = 10^2$–$10^4$ (Osterbrock 1989). Thus an effect due to the decrease in optical depth with time is probably indicated. Because the He I lines originate in at least two distinct regions, the temporal changes may be more pronounced in the broader line region.

#### *4.2.3 The Balmer lines*

It has already been noted that the Balmer lines have a complex structure which evolves with time. At the discovery, only weak narrow lines are present, probably of circumstellar origin. More than one month later, a more complicated structure is already apparent.

In fact, an adequate fit of the H$\alpha$ profile, which is the strongest feature of the spectrum at 115 d, requires at least three Gaussian components: an unresolved, an intermediate (FWHM $\simeq 2200$ km s$^{-1}$) and a broad one (FWHM $\simeq 15\,000$ km s$^{-1}$). Fig. 7 shows this deconvolution. It should be noted here that, although a Gaussian fit gives FWHM = 15 000 km s$^{-1}$, the velocities of the broad component at zero intensity may exceed 20 000 km s$^{-1}$. At later phases, the unresolved component is not required for a satisfactory fit of the H$\alpha$ profile, while the two broadest components remain visible for 3 yr. H$\beta$ also has two components, the former unresolved and the latter with FWHM ~ 2500 km s$^{-1}$. If a broader

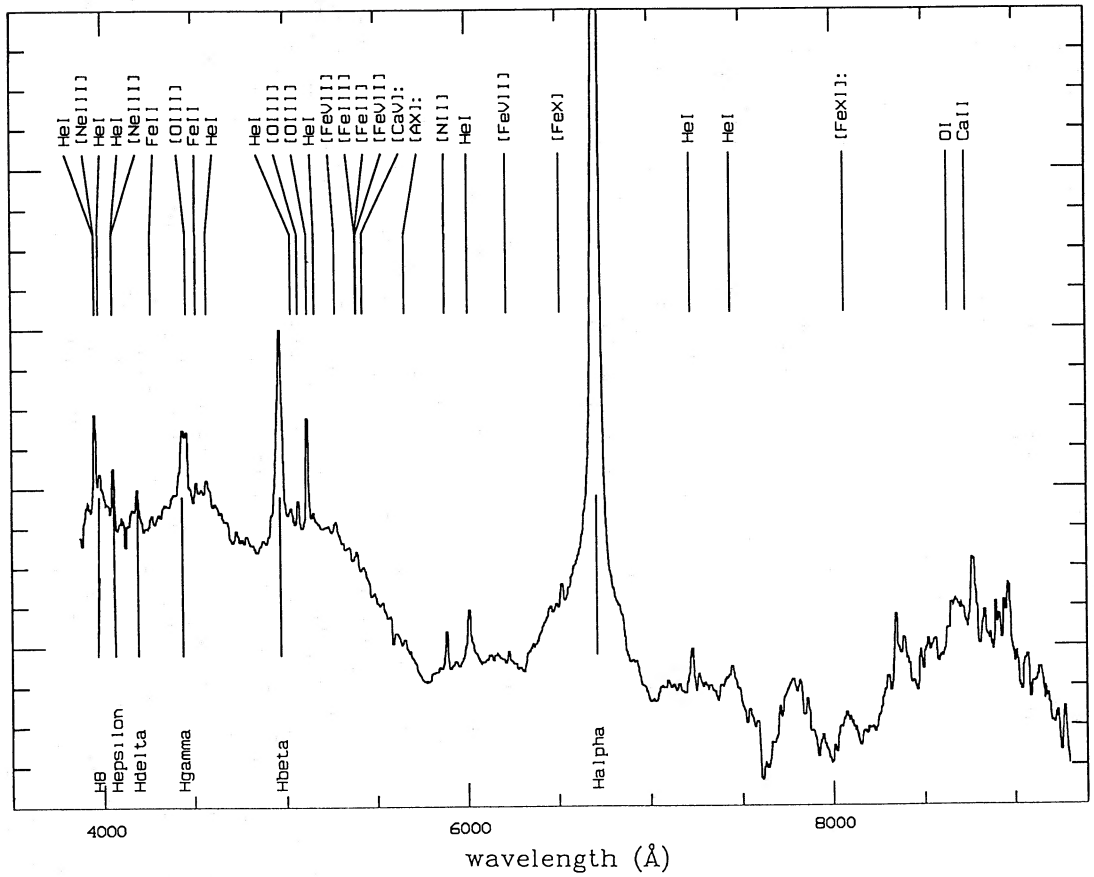


**Figure 6.** Line identifications on the spectrum at day 115.

**Table 4.** Emission-line identifications and fluxes.

| Ion | $\lambda_o$ | line | rest wavelength (Å) | | | | | total intensity ($10^{-16}$ erg s$^{-1}$ cm$^{-2}$) | | | | |
|---|---|---|---|---|---|---|---|---|---|---|---|---|
| | | shape | 115$^d$ | 492$^d$ | 738$^d$ | 798$^d$ | 1149$^d$ | 115$^d$ | 492$^d$ | 738$^d$ | 798$^d$ | 1149$^d$ |
| [NeIII],HeI | 3869,3867 | blend | 3866 | 3863 | 3868 | 3946 | | 21 | | 5 | 3 | |
| $H_8$,HeI | 3889,3889 | blend | 3894 | 3887 | | | | 4 | | | | |
| $H_\epsilon$,[NeIII],HeI | 3970,3968,3965 | blend | 3967 | | 3966 | 3961 | 3962 | 13 | | 2 | 2 | 1 |
| $H_\delta$ | 4102 | – | 4098 | | 4097 | | 4097 | 7 | | 3 | | 1 |
| FeII | 4173,4178 | – | 4177 | | | | | 3 | | | | |
| $H_\gamma$ | 4340 | blend | 4342 | 4333 | 4334 | 4340 | 4335 | 26 | 18 | 5 | 5 | 4 |
| [OIII] | 4363 | blend | 4361 | 4348 | 4357 | | | 8 | 3 | 2 | | |
| FeII | 4417 | – | 4416 | | | | | 2 | | | | |
| HeI | 4472 | – | 4471 | 4465 | 4473 | | 4467 | 3 | 3 | 1 | | 1 |
| $H_\beta$ | 4861 | complex | 4858 | 4855 | 4856 | 4857 | 4855 | 104 | 106 | 26 | 27 | 8 |
| HeI | 4922 | – | 4920 | 4927 | | | 4922 | 9 | 3 | | | 0.4 |
| | | broad | | 4961 | 4956 | 4961 | 4960 | | 217 | 52 | 29 | 12 |
| [OIII] | 4959 | narrow | 4958 | 4954 | 4953 | 4956 | 4954 | 6 | 5 | 1 | 3 | 1 |
| [OIII] | 5007 | narrow | 5006 | 5003 | 5001 | 5004 | 5004 | 26 | 52 | 7 | 8 | 5 |
| HeI | 5048 | – | 5039 | 5041 | | | 5038 | 2 | 4 | | | 0.3 |
| [FeVII] | 5158 | – | 5155 | 5164 | 5165 | 5157 | 5159 | 3 | 10 | 4 | 2 | 2 |
| | | broad | | 5237 | 5227 | | | | 89 | 16 | | |
| [FeII],[FeIII],[FeVII] | 5269+5273,5270,5276 | – | 5271 | | 5266 | 5270 | 5272 | 4 | | 1 | 2 | 2 |
| [CaV]: | 5309 | – | | 5309 | 5310 | 5314 | 5311 | | 6 | 1 | 2 | 2 |
| [AX]: | 5535 | – | 5528 | | | | | 2 | | | | |
| [NII] | 5755 | narrow | 5755 | 5754 | 5754 | 5757 | 5750 | 9 | 4 | 4 | 4 | 1.2 |
| HeI | 5876 | complex | 5878 | 5873 | 5874 | 5874 | 5872 | 21 | 28 | 12 | 9 | 5 |
| [FeVII] | 6086 | – | 6090 | 6088 | 6086 | 6095 | 6082 | 2 | 3 | 1 | 3 | 1 |
| [FeX] | 6373+6375 | – | 6377 | 6373 | 6373 | | 6368 | 5 | 4 | 2 | | 0.5 |
| $H_\alpha$ | 6563 | complex | 6566 | 6559 | 6559 | 6560 | 6558 | 1294 | 1738 | 652 | 727 | 301 |
| HeI | 7065 | – | 7066 | 7063 | | | 7052 | 14 | 3 | | | 1 |
| HeI | 7281 | – | 7281 | | | | 7296 | 3 | | | | 3 |
| [FeXI]: | 7889+7892 | – | 7897 | | | | | 2 | | | | |
| OI | 8446 | broad | | 8436 | | 8455 | 8440 | | 292 | | 30 | 4 |
| CaII | 8498,8542,8662 | broad | 8514 | | | | | 900 | | | | |

component exists, it is not visible, indicative of a steep decrement. H$\gamma$ is blended with [O III], making the deconvolution of this structure very difficult.

For all the spectra with signal-to-noise ratios sufficient to distinguish more than one component, Table 5 lists the widths of the different components of H$\alpha$, H$\beta$ and He I, corrected for the instrumental width determined on the night-sky emissions. The fit has been performed independently by means of the SLP program (Pegoraro 1990) and a different MIDAS procedure. Although the result of the fitting is not univocal, it is reassuring that both procedures reach similar results with the same number of components and that the characteristics of the various components are nearly coincident.

**Table 5.** H and He I line components.

| epoch | FWHM (km s$^{-1}$) | | | | | | |
|---|---|---|---|---|---|---|---|
| | H$\alpha$ | | | H$\beta$ | | HeI(5876 Å) | |
| | broad | interm. | narrow | interm. | narrow | interm. | narrow |
| 115 | 14952 | 2205 | <700 | 2476 | <800 | 2149 | <700 |
| 492 | 5138 | 1648 | | 2159 | <1200 | 2332 | <1200 |
| 684 | 5794 | 1495 | | | | | |
| 717 | 6325 | 1455 | | | | | |
| 738 | 4352 | 1400 | | 2122 | <1200 | 2874 | <1200 |
| 758 | 5137 | 1278 | | | | | |
| 798 | 5022 | 1580 | | 1395 | <800 | 1710 | <800 |
| 1149 | 5740 | 1415 | | 984 | <800 | 1799 | <800 |

| epoch | intensity ($10^{-16}$erg s$^{-1}$ cm$^{-2}$) | | | | | | |
|---|---|---|---|---|---|---|---|
| | H$\alpha$ | | | H$\beta$ | | HeI(5876 Å) | |
| | broad | interm. | narrow | interm. | narrow | interm. | narrow |
| 115 | 624 | 517 | 153 | 96 | 8 | 15 | 6 |
| 492 | 281 | 1457 | | 61 | 50 | 23 | 5 |
| 684 | 116 | 794 | | | | | |
| 717 | 134 | 702 | | | | | |
| 738 | 109 | 543 | | 23 | 4 | 8 | 5 |
| 758 | 105 | 693 | | | | | |
| 798 | 86 | 641 | | 24 | 3 | 7 | 2 |
| 1149 | 25 | 277 | | 7 | 2 | 4 | 1 |

The broadest component of H$\alpha$, as measured in our spectra, shows a slow but unambiguous evolution. The FWHM velocity decreases from 15 000 km s$^{-1}$, at 115 d, to about 5000 km s$^{-1}$ at 2 yr after outburst. Moreover, its central position drifts redwards. At 115 d, we measure a blueward displacement with respect to the unresolved component of about 2500 km s$^{-1}$. At phase 500 d it has decreased to about 900 km s$^{-1}$, and at 1150 d to 600 km s$^{-1}$. It should be noted that such evolution is not perceptible in the data presented by SS, where both the expansion velocities and the position of the broadest H$\alpha$ component appear nearly constant. We note, however, that for the late spectra, where the broad component is weak, the fitting procedure becomes somewhat arbitrary, thus making the conclusion more qualitative than quantitative. Nevertheless, this effect is what one might expect if the envelope is initially optically thick, with H$\alpha$ formed mostly in the outer layers, and then becomes increasingly optically thin as the envelope expands.

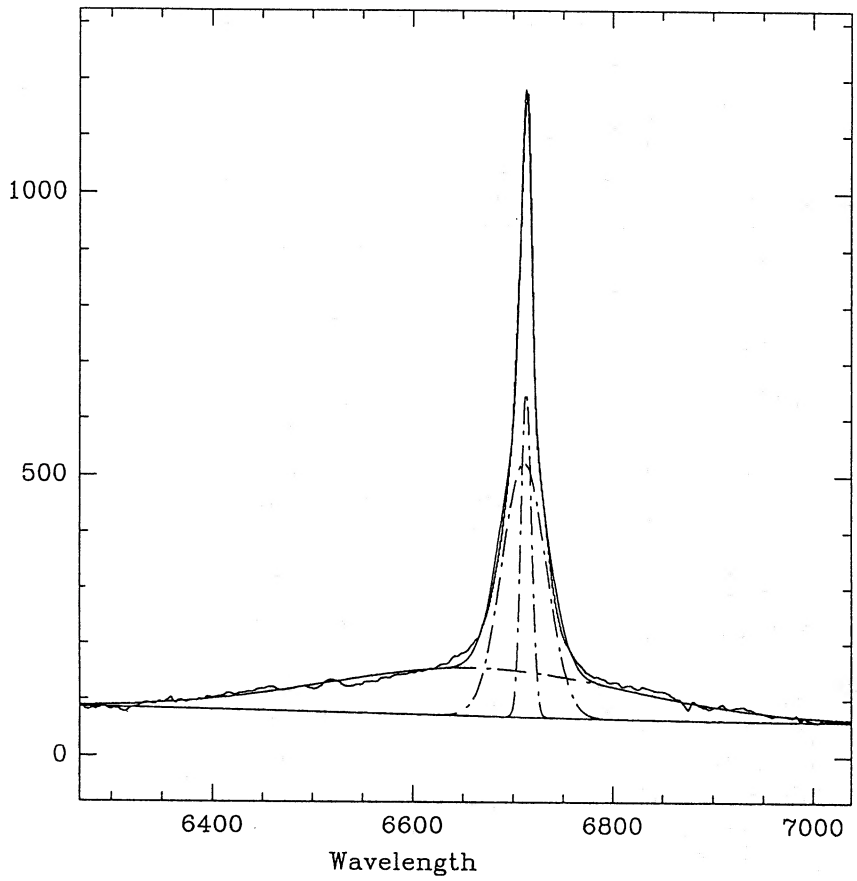


**Figure 7.** The deconvolution into three components of the profile of H$\alpha$ at phase 115 d. The parameters of the three components are given in Table 5. The dot-dashed lines represent the single components, while the solid lines represent the global fit and the observed profile.

The intermediate component also shows clear temporal evolution. From the time of its early detection (45 d after the discovery) until about 100 d it maintains an expansion velocity of about 2000–2500 km $s^{-1}$. Later this decreases to 1400 km $s^{-1}$ at 1150 d. The corresponding components of H$\beta$ and He I behave similarly.

Decomposition also allows one to measure the fluxes of the components. They are reported in Table 5, while Fig. 8 shows their temporal luminosity evolution together with results for other supernovae.

The Balmer decrement is very steep and becomes steeper with time. The total line ratio H$\alpha$/H$\beta$ is 12.4 at phase 115 d, rising to about 37 at phase 1150 d. The single-component ratios also become steeper with time.

#### 4.2.4 *The lower excitation forbidden lines*

The optical spectrum is also characterized by several intense forbidden lines of [O III], [Ne III] and [N II], all of which *remain unresolved at all phases*. Thus the velocity of the material where they form is lower than 700 km $s^{-1}$. The [O III] 4959–5007- and 4363-Å and the [N II] 5755-Å lines are the strongest, the intensities of which change with time, revealing that they are associated with the SN event rather than with some foreground or background source.

It has already been noted by SS that the intensity ratio of [O III] 4959+5007 to [O III] 4363 Å, used in gaseous nebulae to determine the electron temperature, is far lower than is possible in the low-density limits. Also, the presence of a strong [N II] 5755-Å line and the non-detection of the 6548- and 6583-Å [N II] lines (in part due to their proximity to the strong broad H$\alpha$ line) indicate a high density for the gas in which the lines form.

#### 4.2.5 *The coronal lines*

When the signal-to-noise ratio of the spectra is sufficiently high, weaker narrow forbidden lines of extremely high ionization, typical of the solar corona, are visible. In particular, we identify [Fe X] 6375, [Fe VII] 5159, [Fe VII] 6086 Å and, more uncertainly, [Fe XI] 7888–7892, [A X] 5535 and [Ca V] 5309 Å. Such a range of coronal lines has not previously been reported in supernova spectra, although some of the lines are now becoming apparent in the spectra of SN 1987A (Danziger et al., in preparation). The [Fe X] 6375-Å line appears to be present (although unremarked) in the spectrum of day 45 presented by SS and remains at least until day 492 in our spectra. The precise temporal evolution remains to be defined. The examination of other late-time SNeII spectra in the literature reveals the presence of such lines (though without identification) in the spectra of SN 1986J (Rupen et al. 1987; Leibundgut et al. 1991).

Coronal lines are typical of recurrent and other novae (e.g. Ferland, Lambert & Woodman 1977; Rosino 1986) and have been interpreted in terms of dissipation of the energy of a shock wave in the circumstellar envelope (e.g. Gorbatskii 1973) or of turbulence within the ejecta (Shields & Ferland 1978). The fact that the [Fe XIV] 5303-Å line is never

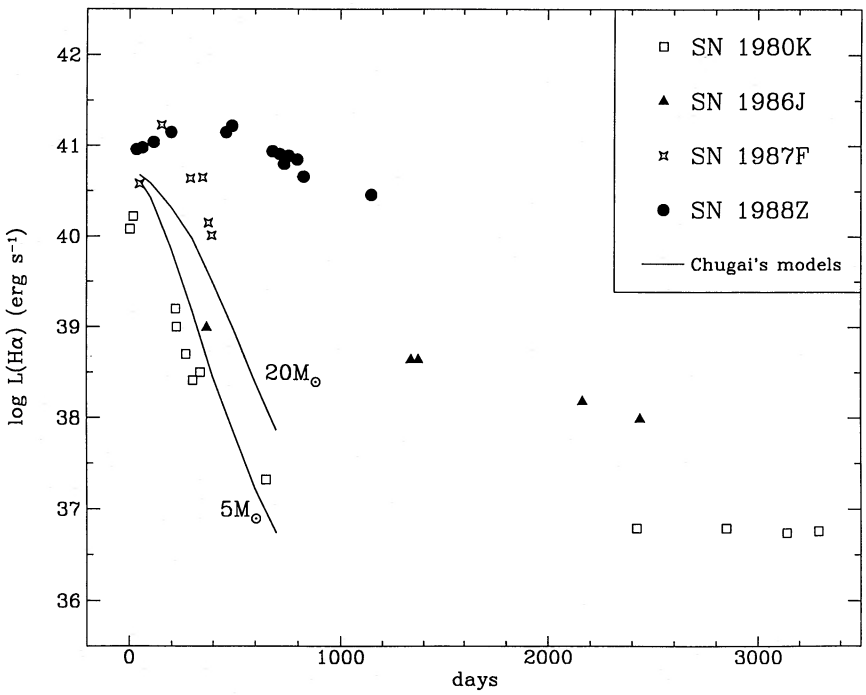


**Figure 8.** The H$\alpha$ luminosity of SN 1988Z as a function of time. The two solid curves are the flux evolution of the one-zone radioactive model of Chugai (1991) with envelope mass $M=5$ and 20 $M_\odot$ and $E=10^{51}$ erg, $M_{Ni}=0.075$ $M_\odot$, $X=0.6$. Data for SN 1980K are from Uomoto & Kirshner (1986), Uomoto (1991), Fesen & Becker (1990) and Leibundgut et al. (1991), while those for SN 1986J are from Leibundgut et al. (1991), and those for SN 1987F are from Filippenko (1989). The data for SN 1988Z refer only to the resolved emissions (broad and intermediate of Table 5) and come from SS and this paper. The spread between the points at contiguous phases is possibly due to errors in the absolute calibration. The adopted distances for SN 1980K, 1986J, 1987F and 1988Z are 5.5, 9.6, 63.4 and 89.8 Mpc, respectively.

detected while, at 115 d, the [Fe x] 6375-Å line is strong allows one to restrict the electron temperature at this phase to $T_e < 2 \times 10^6$ K (Jordan 1969). The intensity ratio of [Fe vii] 6087 to [Fe x] 6374 Å appears to evolve with time and, at phase 798 d, the [Fe x] line is no longer visible. This suggests that the electron temperature has diminished to $T_e \sim 2 \times 10^5$ K.

## 5 DISCUSSION

The light curves of SN 1988Z in the three optical bands are unusual (Fig. 2). At early epochs, although a definite flat plateau like that in SN 1969L was not seen (Fig. 3), there is no doubt that the curves are relatively broad. Theoretical models (e.g. Swartz, Wheeler & Harkness 1991) need progenitors with large, extended envelopes to give broad light curves.

At greater ages of the SN, the luminosity evolves particularly slowly. Unlike other SNeII, between 150 and 400 d the luminosity decline is significantly slower (e.g. $\gamma_R = 0.18$) than the decay rate of the $^{56}$Co ($\gamma = 0.99$). Some additional source of energy is therefore required to power the SN. This extra source is required to be effective up to 3 yr after explosion.

Lacking observations of our own, for the spectra of SN 1988Z near maximum we refer to Filippenko (1991). The spectrum is characterized by a blue continuum with very narrow Balmer and [O iii] emission lines, quite different from the typical spectra of normal SNeII and from those of SN 1987A, which were dominated by broad P Cyg lines of hydrogen and other intermediate-weight elements of the stellar atmosphere.

Type II SN spectra have been successfully modelled in the past. Impressive fits of the observed spectra of SN 1987A were obtained by Lucy (1987), Fosbury et al. (1987) and Danziger et al. (1988), who applied an escape-probability model with an approximately NLTE treatment. It is clear that these models alone are not applicable to the spectra of SN 1988Z.

Schlegel (1990) included SN 1988Z in a new subclass of SN, the SNIIn, which share several properties at maximum light such as the blue continuum, a broad H$\alpha$ emission with no P Cyg profile and a narrow peak which, according to Schlegel (1990), is probably due to a surrounding H ii region.

The most detailed study of a SN of this class concerns SN 1987F (Filippenko 1989), whose resemblance to SN 1988Z is striking in some respects. Apart from the previously mentioned characteristics, there is the persisting presence of the 5876-Å He i line and the weakness (absence in SN 1988Z) of the typical [O i] and [Ca ii] lines at late time. Common properties also include the broad shape of the light curves and the bright absolute magnitude (see Section 3.2).

There are, however, noticeable differences between the two objects. We showed before that for SN 1988Z the narrow emission lines are intrinsic to the SN, while in the SN 1987F they probably arise from a surrounding H ii region (Filippenko 1989). In the spectra of SN 1988Z, we have identified neither strong Fe ii nor Na i features, which are apparent in SN 1987F. The colour curves are also different (Fig. 4).

Since many of the observed features of the SNe which Schegel (1990) included in this new class are probably due to the interaction of the expanding envelope with the circumstellar medium (CSM), a wide degree of individuality is expected, because of possible differences in the density structures of the envelope and in the density and spatial distribution of the CSM/ISM, as well as in the expansion velocity of the envelope. Therefore, at this stage, it is not clear whether all SNe of this class are physically related through a similar progenitor.

At late times, the spectra of SN 1988Z are also very different from those of other SNeII. In all our spectra, as well as those by SS, several unresolved lines have been noted near the velocity of the galaxy. These lines are relatively bright. The fact that the intensities of these lines decrease precludes the possibility that they are a contamination by adjacent emission-line regions.

Such narrow lines have been seen in other SNeII, e.g. SN 1979C (Branch et al. 1981), SN 1984E (Dopita et al. 1984) and SN 1987A (Wampler, Richichi & Baade 1989). It is probable that the material lost by the progenitor as a slow stellar wind has been excited by the pulse of energetic photons which follows the core collapse, in analogy to SN 1987A (Lundqvist & Fransson 1991). In Section 4 we showed that in the case of SN 1988Z the CSM has a very high density.

Stathakis & Sadler (1991) showed that between two and four months after maximum the Balmer decrement of the narrow-line component changes from 7 to 19. For the two broader components combined, we refer to our data. The H$\alpha$/H$\beta$ ratio changes from 12 to 34 between phases 115 and 1150 d. It is therefore probable that in SN 1988Z the collisional excitation increases with the phase, as suggested by Branch et al. (1981) for SN 1979C.

Of interest for an understanding of the phenomenology of SN 1988Z at late phases is the work of Chugai (1991). According to his hypothesis, the additional source of energy necessary to reproduce the observed behaviour of H$\alpha$ (the strength of which exceeds that expected from a simple radioactive model) of this type of SN is supplied by the release of mechanical energy due to the interaction of the SN ejecta with the circumstellar wind, characteristic of SNe whose progenitors experienced strong stellar winds before the explosion. Other properties shared by the H$\alpha$-excess SNe, namely the high velocity of the H$\alpha$-emitting material, the presence of a narrow component and the absence of blue-shifted absorption, can be explained by this theory.

Among the objects considered by Chugai (1991), SN 1987F showed the largest departure from the radioactive model. It is this object which shows the strongest similarity to 1988Z. The H$\alpha$ flux of SN 1987F shows an increase between 50 and 150 d and a subsequent fast decline. This fluctuation should be treated with care because of possible uncertainties in the absolute flux calibration. Nevertheless, a real excess over that expected from the radioactive model is apparent.

We show on the same plot (Fig. 8) the H$\alpha$ fluxes of SN 1988Z from Table 5 and from SS, together with Chugai's radioactive models with 5 and 20 $M_\odot$. The fluxes of SN 1988Z remain even higher than those of SN 1987F. Moreover, unlike those of other SNeII, the H$\alpha$ fluxes of SN 1988Z have an extremely low variation over the whole period studied here. It is clear that, because the two radioactive models do not approximate the SN behaviour, SN

1988Z is the most outstanding candidate for a supernova undergoing the process invoked by Chugai (1991), i.e. energy release due to an ejecta–wind interaction.

Of the supernovae that show characteristics indicative of ejecta–wind interaction, Chugai (1991) has drawn attention to SN 1979C and 1980K as having radio emission. Since this is to be expected on theoretical grounds from a shock wave propagating in a dense circumstellar wind, it should be noted that SN 1988Z has also been detected at radio frequencies (Sramek, Weiler & Panagia 1990). Although details have not yet been published, it apparently reached a radio luminosity similar to that of SN 1986J, the most luminous radio SN ever detected. That being so, it is worth noting the characteristics that SN 1988Z and SN 1986J have in common. This latter SN was discovered in the radio and subsequently detected at optical wavelengths on CCD frames taken more than 2 yr earlier. Some similarities of this object to SN 1988Z have already been noted by Leibundgut (1991) on the basis of the slow fading rate, the late H$\alpha$ flux and the radio emission.

An extensive study of SN 1986J (Leibundgut et al. 1991) showed that it had two components of emission, but that these were reversed with respect to 1988Z: narrow lines of H, He, N and Fe and broader lines of [O I], [O II] and [O III]. H$\alpha$ declined very slowly between 2 and 7 yr after maximum. This behaviour was interpreted as the explosion of a massive star surrounded by dense circumstellar material formed by the star as a result of a stellar wind. The broad lines are emitted by the H-depleted ejecta, while the narrow ones arise in the slowly expanding circumstellar material. Our identification of coronal lines in the spectra of SN 1986J supports this scenario. The basic similarity is therefore the presence of an ejecta–wind interaction. A probable difference is in the nature of the progenitor stars.

## 6 CONCLUSIONS

The present work is based on observations obtained between 3 and 40 months after the discovery of SN 1988Z, which, together with other observations reported in the literature, confirm, strengthen and enlarge our knowledge of supernova interactions with nearby material formed by a wind.

The broad light curve around maximum light indicates that the progenitor star had an extended envelope. Although rather bright, the luminosity at maximum is not exceptional. Nevertheless, because of the slow fading rate, the SN develops an increasingly large excess by comparison with other SNeII at the same phase. The slow light decay at late stages, now extending beyond 1150 d, implies that the light curves are not powered by the radioactive decay of $^{56}$Co alone, but that some additional source of energy is required. The colour evolution is unique. Contrary to the normal pattern for SNeII, 1988Z moves from an initial $(B-V)\simeq 0.4$ towards the blue colour until about 100 d, settling at later phases at $(B-V)\simeq 0.65$. This blue colour is obviously associated with the peculiar rise of the spectrum in the region 3500–5700 Å; it is suspected that this rise is caused by the overlap of a huge number of emission lines formed in the envelope.

Several forbidden lines, including coronal lines, characterize the spectrum at late epochs. All are unresolved, indicating that emitting material is slower than 700 km s$^{-1}$. The line-intensity ratios show that the electron density is higher than in the low-density regime. All of these seem to evolve with time.

The Balmer lines have a complex structure which also evolves with time. They are formed by several components of emission and there is never any sign of the P Cygni absorption typical of SNeII, a signature of the fact that H$\alpha$ emission is largely confined to an outer shell. Shortly after the discovery, only weak, narrow emission lines are visible on the continuum. With the passage of time, two broader components (FWHM $\simeq$ 20 000 and FWHM $\simeq$ 2000 km s$^{-1}$) emerge. At the very late phases, the spectrum is dominated by a sole intermediate component, the other two having practically disappeared. The total H$\alpha$ luminosity has a slow evolution and does not fit the one-zone radioactive model. These features, along with the above-mentioned properties of the H$\alpha$ emission, mean that SN 1988Z is one of the best candidates for a supernova in which there is an interaction of SN ejecta with the circumstellar wind (Chugai 1991).

The presence of coronal lines suggests the presence of a shock. Though relatively weak, the lines have been unambiguously identified in the spectra of SN 1988Z. Such lines are also probably present in the optical spectra of SN 1986J, for which an extended dense circumstellar environment has been invoked to explain the radio and the optical observations (Weiler, Panagia & Sramek 1990; Leibundgut et al. 1991). SN 1988Z is also a strong radio source. These features further support the concept of an ejecta–wind interaction.

Continuing studies of this type of supernova are important from the point of view of theories of active galactic nuclei. For example, in a recent paper, Terlevich et al. (1992) have proposed a model of AGN in which the energy output is provided by the expansion of supernova remnants into a dense circumstellar medium. It is interesting and suggestive that the integrated H$\alpha$ flux in the first 2.5 yr for this model (taken from their table 2) shows good agreement with that in our results (presented in Fig. 8). Fig. 2 of the Terlevich et al. (1992) paper demonstrates that there is predictive power in their model because the H$\alpha$ flux passes through a strong sharp maximum after ~3 yr. Although our last observation, plotted in Fig. 8, coincides with this epoch, no idnication of an increase in the luminosity of H$\alpha$ is apparent. Nevertheless, this provides an additional incentive to continue to observe SN 1988Z and similar supernovae over long intervals of time. Filippenko (1989) made comparisons between the spectra of supernovae other than SN 1988Z and those of AGN. A cursory comparison of the early spectrum of SN 1988Z with an average quasar spectrum is not strongly suggestive. Nevertheless, if the blue excess in SN 1988Z discussed above can be partially or wholly modelled with the involvement of allowed and forbidden transitions of Fe II, this will go some way towards strengthening the above theory of AGN spectra.

## ACKNOWLEDGMENTS

We are indebted to Professor L. Rosino for stimulating discussions.

## REFERENCES

Barbon R., Ciatti F., Rosino L., Ortolani S., Rafanelli P., 1982, A&A, 116, 43

Benetti S., Cappellaro E., Turatto M., 1991, A&A, 247, 410
Bouchet P., Danziger I. J., Lucy L. B., 1991, in Danziger I. J., Kjär K., eds, ESO Workshop Conf. Proc. No. 37, SN 1987A and other Supernovae. ESO Garching, p. 281
Branch D., Falk S. W., McCall M. L., Rybski P., Uomoto A. K., Wills B., 1981, ApJ, 244, 780
Burstein D., Heiles C., 1978, ApJ, 225, 40
Cappellaro E., Turatto M., 1988, IAU Circ. 4691
Chugai N. N., 1991, MNRAS, 250, 513
Ciatti F., Rosino L., Bertola F., 1971, Mem. Soc. Astron. Ital., 42, 163
Danziger I. J., Bouchet P., Fosbury R. A. E., Gouiffes C., Lucy L. B., Moorwood A. F. M., Oliva E., Rufener F., 1988, in Kafatos M., Michalitsianos A., eds, SN 1987A in the LMC. Cambridge Univ. Press, Cambridge, p. 37
Danziger I. J., Bouchet P., Gouiffes C., Lucy L. B., 1989, IAU Circ. 4746
Dopita M., Evans R., Cohen M., Schwartz R. D., 1984, ApJ, 287, L69
Ferland G., Lambert D. L., Woodman J. H., 1977, ApJ, 213, 132
Fesen R. A., Becker R. H., 1990, ApJ, 351, 437
Filippenko A. V., 1989, AJ, 97, 726
Filippenko A. V., 1991, in Danziger I. J., Kjär K., eds, ESO Workshop Conf. Proc. No. 37, SN 1987A and other Supernovae. ESO, Garching, p. 343
Fosbury R. A. E., Danziger I. J., Lucy L. B., Gouiffes C., Cristiani S., 1987, in Danziger I. J., ed., ESO Workshop Conf. Proc. No. 26, SN 1987A. ESO, Garching, p. 139
Gorbatskii V. G., 1973, SvA, 17, 11
Grandi S. A., 1980, ApJ, 238, 10
Heathcote S., Cowley A., Hartwick D., 1988, IAU Circ. 4693
Jordan C., 1969, MNRAS, 142, 501
Landolt A. U., 1983, AJ, 88, 439
Leibundgut B., 1991, in Danziger I. J., Kjär K., eds, ESO Workshop Conf. Proc. No. 37, SN 1987A and other Supernovae. ESO, Garching, p. 363
Leibundgut B., Kirshner R. P., Pinto P. A., Rupen M. P., Smith R. C., Gunn J. E., Schneider D. P., 1991, ApJ, 372, 531
Lucy L. B., 1987, in Danziger I. J., ed., ESO Workshop Conf. Proc. No. 26, SN 1987A. ESO, Garching, p. 417
Lucy L. B., Danziger I. J., Gouiffes C., Bouchet P., 1989, in Tenorio-Tagle G., Moles M., Melnick J., eds, Structure and Dynamics of the Interstellar Medium. Springer-Verlag, Berlin, p. 164
Lundqvist P., Fransson C., 1991, ApJ, 380, 575
Miller D. L., Branch D., 1990, AJ, 100, 530
Oliva I., Moorwood A. F. M., Danziger I. J., 1987, The Messenger, 50, 18
Osterbrock D. E., 1989, Astrophysics of Gaseous Nebulae and Active Galactic Nuclei. University Science Books, Mill Valley, CA
Patat F., 1992, Doctoral thesis, Universitá di Padova
Pegoraro A., 1990, Internal Report 2, Oss. Astron. Padova
Pollas C., 1988, IAU Circ. 4691
Rosino L., 1986, in Bode M. F., ed., R. S. Ophiuchi (1985) and the Recurrent Nova Phenomenon. VNU Science Press, Utrecht, p. 1
Rupen M. P., van Gorkom J. H., Knapp G. R., Gunn J. E., 1987, AJ, 94, 61
Schlegel E. M., 1990, MNRAS, 244, 269
Shields G. A., Ferland G. A., 1978, ApJ, 225, 950
Sramek R. A., Weiler K. W., Panagia N., 1990, IAU Circ. 5112
Stathakis R. A., Sadler E. M., 1991, MNRAS, 250, 786 (SS)
Suntzeff N. B., Bouchet P., 1990, AJ, 99, 650
Swartz D. A., Wheeler J. C., Harkness R. P., 1991, ApJ, 374, 266
Terlevich R., Tenorio-Tagle G., Franco J., Melnick J., 1992, MNRAS, 255, 713
Turatto M. et al., 1990a, The Messenger, 60, 15
Turatto M., Cappellaro E., Barbon R., Della Valle M., Ortolani S., Rosino L., 1990b, AJ, 100, 771
Uomoto A., 1991, AJ, 110, 1275
Uomoto A., Kirshner R. P., 1986, ApJ, 308, 685
Wampler E. J., Richichi A., Baade D., 1989, in Tenorio-Tagle G., Moles M., Melnick J., eds, Structure and Dynamics of the Interstellar Medium. Springer-Verlag, Berlin, p. 180
Weiler K. W., Panagia N., Sramek R. A., 1990, ApJ, 364, 611
Whitelock P. A., 1991, in Danziger I. J., Kjär K., eds, ESO Workshop Conf. Proc. No. 37, SN 1987A and other Supernovae. ESO, Garching, p. 301
Zamorano J., 1988, IAU Circ. 4694